ELSEVIER

International Journal of Mass Spectrometry 185/186/187 (1999) 813–823

International Journal of Mass Spectrometry

Kinetic energy release for metastable fullerene ions

S. Matt, M. Sonderegger, R. David, O. Echt[1], P. Scheier, J. Laskin[2], C. Lifshitz[2], T.D. Märk*

Institut für Ionenphysik, Leopold Franzens Universität, Technikerstr. 25, A-6020 Innsbruck, Austria

Received 13 July 1998; accepted 16 September 1998

Abstract

Kinetic energy release distributions for spontaneous (metastable) decay of fullerene ions, C_n^{z+}, have been determined for parent sizes $n = 58$, 60, and 70, and charge states $z = 1$, 2, 3, and 4. Extensive numerical modeling has been applied to verify that the shapes of fragment ion peaks in our mass-analyzed ion kinetic energy (MIKE) spectra are not affected by discrimination, making it possible to derive the center-of-mass total kinetic energy release distributions directly from the spectra. Measurements involving $C_3H_8^+$ and $C_3H_7^+$ ions confirm the accuracy of the approach. (Int J Mass Spectrom 185/186/187 (1999) 813–823) © 1999 Elsevier Science B.V.

Keywords: Fullerenes; Propane; Kinetic energy release (KER); Metastable decay; Mass-analyzed ion kinetic energy (MIKE); Dissociation energy

1. Introduction

Mass spectrometric analysis of spontaneous (metastable) reactions of atomic cluster ions has provided a wealth of information about these intriguing species [1]. Surprisingly few studies, however, have attempted to unravel cluster energetics through the analysis of kinetic energy release (KER). Notable exceptions are the analysis of metastable argon and molecular cluster ions employing either time-of-flight or double focusing magnetic sector field instruments (see [2–4], and references therein), and the more recent analysis of metastable carbon cluster ions [5–11]. One objective of this approach is to determine the dissociation energy of cluster ions, another one is the question of whether the dissociation channel involves a reverse activation barrier that, in turn, would carry microscopic information about the dissociation mechanism. The question is particularly pertinent to C_2 emission from fullerenes where several competing mechanisms have been proposed ([12–14], and references therein).

Identification of a reverse activation barrier obviously requires measurement of the kinetic energy release *distribution*. On the other hand, a mere determination of the *average* total kinetic energy release (in the center-of-mass system) might seem to carry

* Corresponding author.

[1] Guest professor at the Institut für Ionenphysik, Innsbruck. Permanent address: Department of Physics, University of New Hampshire, Durham NH 03824-3568.

[2] Department of Physical Chemistry and The Farkas Center for Light Induced Processes, The Hebrew University of Jerusalem, Jerusalem 91904, Israel.

Dedicated to Professor Michael T. Bowers on the occasion of his 60th birthday.

PII S1387-3806(98)14196-9

adequate information about the cluster binding energy. This approach has in fact been pursued in a number of studies [3,4,15]. However, as pointed out by Klots [16,17], the relation between average energy release and binding energy is not unique; it is also affected by angular momentum, moments of inertia, and the interaction between the separating fragments. Only knowledge of the complete kinetic energy release distribution will permit a model-free determination of binding energies.

In this article we present a comprehensive analysis of metastable peaks in mass-analyzed ion kinetic energy (MIKE) spectra of fullerene ions. The KER distributions are determined for the following reactions:

$$C_{58}^{z+} \rightarrow C_{56}^{z+} + C_2 \text{ for } z = 1, 2, 3 \quad (1)$$

$$C_{60}^{z+} \rightarrow C_{58}^{z+} + C_2 \text{ for } z = 1, 2, 3, 4 \quad (2)$$

$$C_{70}^{z+} \rightarrow C_{68}^{z+} + C_2 \text{ for } z = 1, 2, 3, 4 \quad (3)$$

Kinetic energy release distributions are derived from MIKE spectra and characterized in terms of a generalized Maxwell–Boltzmann distribution:

$$f(\epsilon) = a\epsilon^l \exp\left(-\frac{\epsilon}{k_B T^{\ddagger}}\right) \quad (4)$$

where ϵ denotes the total KER in the center-of-mass system. $T^{\ddagger}$ is the temperature of the transition state, k_B is Boltzmann's constant, and a is an arbitrary normalization constant. The a priori unknown exponent l is bound by the relation [16] $0 \leq l \leq 1$; a Gaussian MIKE peak is equivalent to $l = 0.5$. For comparison, and in cases where the statistical quality of the spectra is insufficient, the more common approach of Gaussian fits to the MIKE spectra is used as well.

Parent ions are prepared with a narrow energy distribution down to 120 meV [18] at a beam energy of 3 keV; their small effect on the fragment ion peak shape is eliminated by deconvolution. Extensive numerical modeling of ion trajectories is carried out in order to determine the effect of instrument geometry, slit widths, beam divergence, etc., on the shape of MIKE spectra.

Furthermore, the accuracy of the procedure is tested by analysis of two well-studied metastable reactions of ions derived from propane [19–21]:

$$C_3H_8^+ \rightarrow C_3H_7^+ + H \quad (5)$$

$$C_3H_7^+ \rightarrow C_3H_5^+ + H_2 \quad (6)$$

that are characterized by a very low average KER [reaction (5)], and by a high average KER reflecting a large reverse barrier [reaction (6)].

2. Experiment

All measurements were carried out with a high resolution double focusing mass spectrometer (Varian MAT CH5-DF) of reversed Nier–Johnson type geometry (see Fig. 1). Ions are extracted from the Nier-type electron impact ion source by a weak electric field and accelerated through a potential of 3 kV into the spectrometer. They pass through the first field-free region (1 ff, length 61 cm), are then momentum-analyzed by a 48.5° magnetic sector field, enter a second field-free region (2ff, length 33.3 cm), pass through a 90° electric sector field, and are finally detected by a channeltron-type electron multiplier operated in the single-ion counting mode. The time intervals at which C_{60}^+ ions pass through the 1ff and 2ff regions are, relative to their time of formation: 7.7, 31.2 μs and 49.0, 60.8 μs.

The ion beam is defined by three slits: the source (or α) slit in 1ff at the focus of the magnetic sector, the β slit in 2ff at the common foci of magnetic and electric sector, and the collector (or exit) slit between the electric sector and the detector, positioned at the focus of the former. The dimensions of these slits have a profound effect on the width and peak shape of parent and fragment ions; this will be discussed later.

Parent ions (mass m_1, charge state z_1) may undergo unimolecular dissociation anytime between their formation and detection:

$$m_1^{z_1+} \rightarrow m_2^{z_2+} + m_3^{z_3+} \quad (7)$$

MIKE spectra are used to identify those reactions that occur in the second field-free region: the magnet is tuned to the mass-to-charge ratio of the parent ion

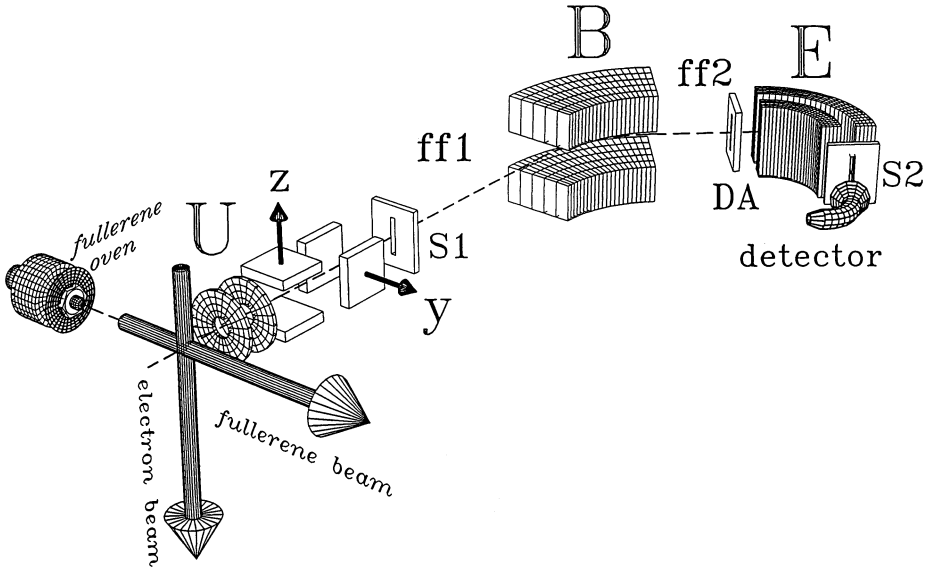

Fig. 1. Schematic view of the experimental setup.

whereas the electric sector field voltage U is scanned [22]. Stable ions (and fragment ions formed in the ion source) will have a kinetic energy of $3z_1$ keV and pass at a sector field voltage of $U_o \approx 509$ V. Daughter ions formed in 2ff via reaction (7), however, will pass at a voltage

$$U = \frac{m_2 z_1}{m_1 z_2} U_o \tag{8}$$

In the present study we are only concerned with reactions that do not involve charge separation, i.e. which have $z_1 = z_2$ and $z_3 = 0$. This makes identification of the daughter mass via Eq. (8) straightforward.

We are mostly interested in kinetic energy distributions of spontaneous (metastable) fragment ions. The low intensity of these signals requires low background pressures in order to avoid collision-induced reactions. In the current experiments, the background pressure was below 3×10^{-8} Torr in the first and second field-free regions.

The present study involves fullerenes and propane. C_{60} powder of 99.99% purity (or C_{70} of 99% purity) is evaporated in a temperature-controlled stainless steel oven typically heated to 950 K. After entering the ion source (background pressure 5×10^{-8} Torr) via a skimmer and collimator, the low-density beam is crossed at right angles by an electron beam of variable energy and current. Alternatively, for measurements involving permanent gases or volatile liquids, vapor is introduced into the collision chamber of the ion source via a conventional capillary gas inlet system.

3. Peak shape analysis

Eq. (8) relates the positions (centroids) of daughter ion peaks formed in 2ff to the position (centroid) of the parent ion peak in a MIKE spectrum. However, the parent ion peak has a finite width and a distinct shape because of the potential gradient in the ion source, and the finite width of slits that define the ion beam. If no kinetic energy were released in reaction (7), the daughter ion peak would have the same shape; its width (relative to that of its parent) would be given by the ratio of sector field voltages, U/U_o.

The kinetic energy released in the reaction will modify the peak shape of the daughter. It is a challenging task to extract the kinetic energy distribution from the fragment ion peak in the MIKE spectrum because instrumental factors may also

greatly affect the peak shape. However, if we ignore, for the moment, all instrumental effects, including the finite width of the parent ion peak, then the procedure is straightforward [23,24]. Consider a parent ion traveling with speed ν_1 through 2ff, dissociating via reaction (7) under release of kinetic energy ϵ [from now on, ϵ will always refer to the *total* kinetic energy release in the *center-of-mass (cm) system*]. The daughter ion of mass m_2 will thus acquire a speed u_2 (in the cm system) given by the relation

$$\epsilon = \frac{m_1 m_2}{2m_3} u_2^2 \tag{9}$$

If the daughter ion is ejected exactly in the forward direction ($\theta = 0$), then the electric sector field voltage required to pass it to the detector is higher than that for a daughter ion released with zero energy by an amount ΔU according to [22]

$$\epsilon = \frac{z_2^2 m_1^2 U_{\mathrm{acc}}}{4 z_1 m_2 m_3} \left(\frac{\Delta U}{U_{\mathrm{o}}} \right)^2 \tag{10}$$

where U_{acc} is the acceleration voltage (3 kV), U_{o} is the electric sector field voltage required to pass the parent ion (509 V), and the other quantities are defined by reaction (7). Strictly speaking, Eq. (10) is only an approximation; it assumes $u_2/\nu_1 \ll 1$. In its more common variant, frequently used to derive an *average* KER from MIKE spectra, ΔU would refer to the difference between ions ejected in the *forward* and *backward* direction; in this case the relation would involve a factor 16 instead of 4 in the denominator, and it would be exact.

The direction of u_2 will usually be isotropic in the cm system. The electric sector field measures the component of the u_2 velocity vector projected onto the forward direction, i.e. ions will be selected according to their value of $(\nu_1 + u_2 \cos\theta)^2$. From this, and Eq. (10), it follows that reaction (7) with a strictly monoenergetic KER distribution will give rise to a MIKE peak that is very nearly [25] rectangular; its edges will be shifted from its centroid by an amount ΔU as given by Eq. (10).

The KER distribution in the cm system can therefore [21,24] be obtained, except for an irrelevant constant factor, by taking the derivative $dI/d(\Delta U)$ over the left or right half of a fragment ion peak in a MIKE spectrum, $I(\Delta U)$. The ΔU values must then be transformed to ϵ with the help of Eq. (10). The procedure is, within its assumptions, valid for any peak shape, but care must be taken to measure ΔU relative to the exact centroid of the fragment peak. A rectangular MIKE peak will, obviously, result in a KER distribution described by a Δ function, whereas a Gaussian peak will yield a distribution as given by Eq. (4) with $l = 0.5$.

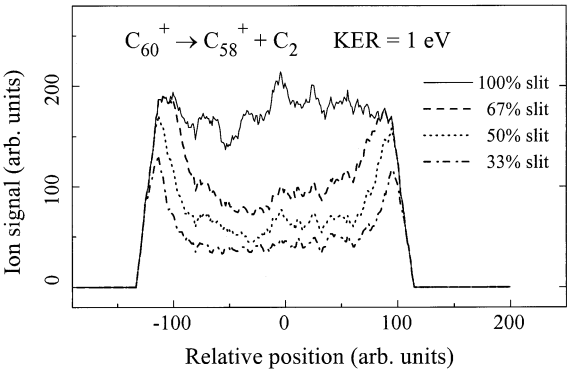

Fig. 2. Simulated MIKE peaks for metastable decay of C_{60}^+ into C_{58}^+, assumed to proceed with a KER of 1 eV. Peak distortion arises from discrimination in the z direction if the length of the collector slit is reduced.

4. Numerical simulations

The KER distribution is easily derived from a metastable peak in the MIKE spectrum only under idealized conditions. In practice, the rectangular peak expected for a monoenergetic metastable reaction will have rounded edges due to finite resolution (finite slit widths, spread of kinetic energy of parent ions, divergence of ion beam, aberrations of magnetic and electric fields), and it may be dished (depressed near the center) due to discrimination. These effects have been studied analytically and numerically [20,23,26], but the results are strongly dependent on the geometry of the mass spectrometer being used, and on the reaction under consideration.

In the present article we explore the effect of slit geometry, beam size, divergence, and KER by numer-

ical simulations. The ion optics program SIMION 3D 6.0 [27] was used to trace trajectories of ions. Fig. 2 displays a simulated MIKE peak of C_{58}^+ fragment ions formed from C_{60}^+ via reaction (2), based on the numerical evaluation of 40 000 individual ion trajectories. Parent ions of 3 keV (monoenergetic) are assumed to travel exactly along the beam axis with zero divergence. Dissociation happens anywhere between the two sector fields with a monoenergetic KER of 1 eV; the location and direction of dissociation are chosen randomly for each event. The resulting MIKE peak (Fig. 2) is approximately flat topped if the full length of the collector slit in the *z* direction is used in the simulation (line labeled "100%"), but significant dishing occurs for reduced slit lengths. (The width of the collector slit, however, is effectively treated as zero, because in the simulation we map the point of arrival of fragment ions in the plane of the collector slit at a fixed sector field voltage, rather than scanning this voltage).

The depression towards the center of the MIKE peak is attributed to those ions that are emitted with a large *z* component (i.e. perpendicular to the beam axis and parallel to the length of the slit) and, thus, miss the collector slit. For a given geometry, the effect depends on the ratio of u_2/v_1. A large KER and small mass ratio of the two fragments, m_2/m_3 (where m_2 refers to the fragment being detected) will lead to increased distortion [see Eq. (9)]. As Fig. 2 demonstrates, reactions (1)–(3) will not suffer from this effect as long as the KER stays below 1 eV and the slit length is set to its maximum. (Dishing will, however, be significant [28] if fragments arise from charge separation reactions which lead to much larger KER values.)

The edges of the simulated MIKE peak in Fig. 2 are rounded because of the finite width of the β slit and because dissociation occurs randomly anywhere between the two sector fields. This effect is explored in more detail in Fig. 3 where the results of four different simulations are shown. Again, decay of C_{60}^+ into C_{58}^+ is modeled, but this time with a monoenergetic KER of only 0.5 eV (close to the experimental, average value of about 0.4 eV, see below). The solid line is obtained if fragment ions are formed at a point

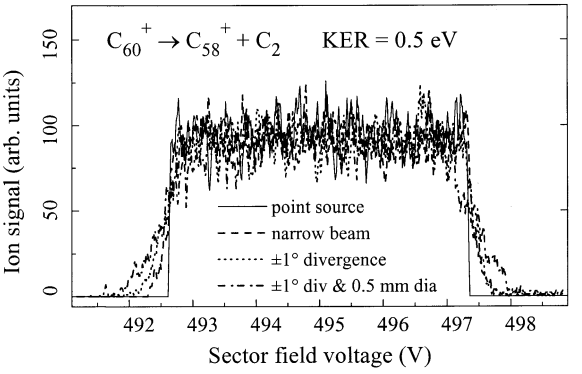

Fig. 3. Simulated MIKE spectra for metastable decay of C_{60}^+ into C_{58}^+, assumed to proceed with a KER of 0.5 eV. Increased broadening is observed when the assumptions about parent ion beam diameter and divergence are relaxed.

in the focal plane (i.e. the β slit) and the parent ion beam has zero divergence; this scenario gives rise to a MIKE peak with very sharp edges. The dashed line (labeled "narrow beam") is obtained if the parent ion beam has zero diameter and zero divergence, but dissociation occurs randomly anywhere in 2ff. The edges of the MIKE peak are broadened further if the parent beam has a finite divergence of $\pm 1°$, but still zero diameter in the focal plane (dotted line). The broadest peak (dash-dotted line) is obtained if, in addition, the beam diameter in the focal plane is set to a finite value of 0.5 mm. Clearly, the last scenario is the most realistic one; it will be used in the following to compare simulated with experimental MIKE peaks.

The derivatives of the simulated MIKE peaks shown in Fig. 3 would result in KER distributions of *finite* width. This problem will be revisited in our discussion of $C_3H_7^+$ decay that features a rather narrow KER distribution. For fullerene ions, however, experimental MIKE spectra do not show any features as distinct as in Fig. 3; in this case a slit width of 0.2 mm appears to provide sufficient resolution to avoid any significant distortions.

5. Kinetic energy release distributions of metastable $C_3H_8^+$ and $C_3H_7^+$

The experimental setup was tested by measuring MIKE spectra of $C_3H_8^+$ and $C_3H_7^+$ parent ions, pro-

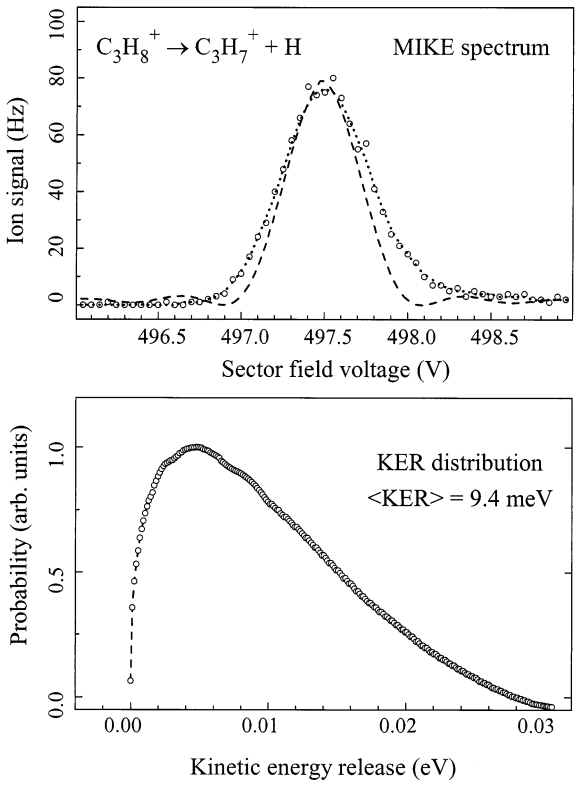

Fig. 4. Results pertaining to the decay of $C_3H_8^+$ into $C_3H_7^+$ + H. The upper panel displays MIKE spectra. Open circles: raw data; dotted line: smoothed data; dashed line: smoothed data deconvoluted with parent ion peak. The bottom panel shows the KER distribution derived from the deconvoluted MIKE spectrum.

duced in the ion source by electron impact ionization of propane:

$$C_3H_8^+ \rightarrow C_3H_7^+ + H \quad (11)$$

$$C_3H_7^+ \rightarrow C_3H_5^+ + H_2 \quad (12)$$

Reaction (11) is accompanied by a very small average KER, on the order of 0.01 eV, thus requiring high resolution and deconvolution with the parent ion peak. Fig. 4 shows the experimental MIKE peak (top panel, open circles), the dotted line represents the data after smoothing. Smoothing as well as deconvolution are based on fast Fourier transform (FFT) techniques [29]. The MIKE peak is very nearly Gaussian, with a relative width [full width at half maximum (FWHM) divided by peak position] of $\Delta U/U = 0.00124$. This value decreases to $\Delta U/U = 0.00097$ after deconvolution (dashed line in Fig. 4). Upon transformation (taking the derivative of the MIKE peak), we obtain a KER distribution as shown in the lower panel in Fig. 4. Its average value is 9.4 meV, in excellent agreement with the value of 9.6 ± 0.3 meV reported by Medved et al. [19].

Careful inspection of the MIKE spectra reveals a slight asymmetry. The peak exhibits a longer tail on the high-energy side, towards the parent ion peak. This effect has been attributed to decays occurring in the electric sector [26]. For this reason, we generally use only the left half of the MIKE peaks to derive KER distributions. The asymmetry limits the accuracy with which the centroid of the peak can be determined. We determine the latter quantity by fitting a Gaussian to the peak over a range which completely includes the left half, but only a small part of the right half. The importance of choosing the correct center of the MIKE peak, as well as the effect of smoothing with FFT filters, will be explored in Sec. 6.

Reaction (12) (metastable decay of $C_3H_7^+$) is well suited to test the quality of the experimental data and the data analysis: the average KER is very close [21,30] to that expected for reactions (1)–(3) (approximately 0.4 eV), and the daughter-to-parent ion mass ratios are also quite similar (41/43 for $C_3H_7^+$ as compared to 58/60 for C_{60}^+). This is important because the extent of any discrimination that might occur at the collector slit for large perpendicular velocity components of u_2 will, as Eq. (9) shows, depend on the KER as well as the mass ratio.

Furthermore, reaction (12) features a reverse activation barrier [21,30] which gives rise to a distinct non-Gaussian MIKE peak. Fig. 5 displays our experimental MIKE spectrum (top, open circles). The dotted line (nearly coincident with the dashed line, see below) presents the result of a nonlinear least-squares fit of a symmetric plateau function with rounded edges. (The function is a product of two generalized Fermi–Dirac distributions, involving four free parameters describing the width, height, centroid, and steepness of the edges.) The experimental MIKE peak is, within the statistical error, flat topped, i.e. there is no

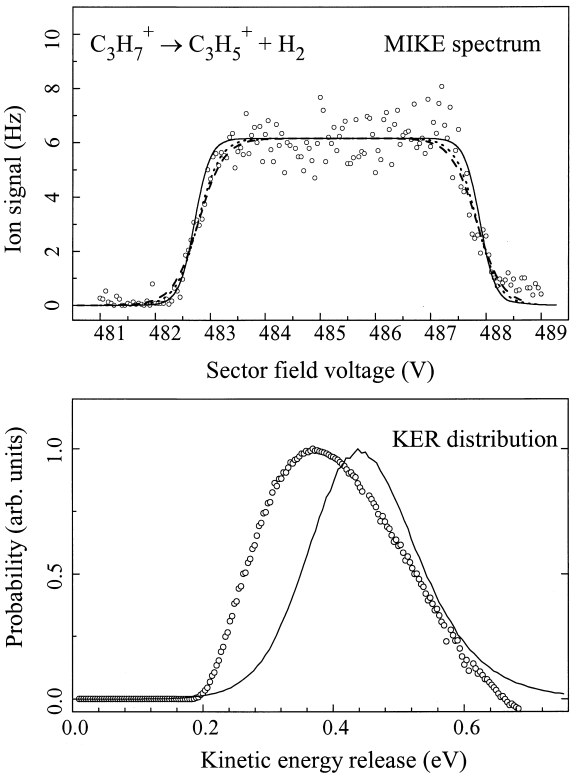

Fig. 5. Results pertaining to the decay of $C_3H_7^+$ into $C_3H_5^+ + H_2$. The upper panel displays MIKE spectra. Open circles: raw data; dotted line: fit to data; solid and dashed lines: fit to simulated MIKE spectra. The lower panel shows KER distributions derived from the deconvoluted experimental data (open circles) and the simulation (solid line).

evidence for any discrimination occurring at the β slit, in agreement with our expectations based on the simulations shown in Fig. 2.

The data are smoothed, deconvoluted with the parent ion peak, and transformed to yield the KER distribution shown in the lower panel in Fig. 5 (open circles). The threshold value of about 0.2 eV (which corresponds to the flat-topped part of the MIKE peak) reflects the existence of a large reverse activation barrier. Generally, the shape of the distribution is in excellent agreement with that reported by Holmes et al. [30]. For example, their distribution peaks at about 0.38 eV while ours peaks at 0.37 eV; their distribution reaches 50% of its maximum at 0.28 and 0.54 eV whereas our corresponding values are 0.26 and 0.53 eV. The average KER values, however, do not agree quite as well; Holmes et al. [21] report 0.44 eV whereas we obtain 0.40 eV. This difference is caused by an apparent distortion of our distribution above 0.6 eV that leads to physically unreasonable negative values above 0.66 eV (our average KER of 0.40 eV refers, in fact, to the energy interval $0.0 \leq \text{KER} \leq 0.66$ eV). The distortion arises in the deconvolution procedure from the application of FFT techniques.

The issue is explored further by simulating MIKE spectra for reaction (12). First, a spectrum is simulated taking into account the finite beam diameter and divergence (Sec. 4) assuming a KER of 0.39 eV. A symmetric plateau function is then fitted to the resulting MIKE spectrum (solid line in Fig. 5, top). The edges of this simulated MIKE spectrum are significantly steeper than those of the experimental data (open circles and dotted line) because a monoenergetic KER was assumed. However, a problem becomes apparent if we transform this simulated MIKE spectrum back into a KER distribution: The rounded edges lead to a distribution of finite width (solid line in Fig. 5, bottom), and the average value of this distribution will exceed the input value of 0.39 eV because of the quadratic dependence of the KER on the sector field voltage [Eq. (10)]. These discrepancies arise from the lack of a proper deconvolution of the simulated MIKE peak.

An alternative procedure, however, can avoid the somewhat ambiguous deconvolution altogether: we use the KER distribution derived from the experimental MIKE spectrum (Fig. 5, bottom, open circles) and approximate it by a histogram. For each energy bin we run ion trajectories with the corresponding (monoenergetic) KER, the number of trajectories being proportional to the bin height. The sum of all these trajectories generates a simulated MIKE spectrum that is based on the experimental KER distribution. A plateau function is fitted to this MIKE spectrum as shown in Fig. 5, top (dashed line). It very nearly coincides with the corresponding curve for the experimental KER spectrum (dotted line). The excellent agreement demonstrates that the experimental KER distribution is, in fact, reasonably accurate.

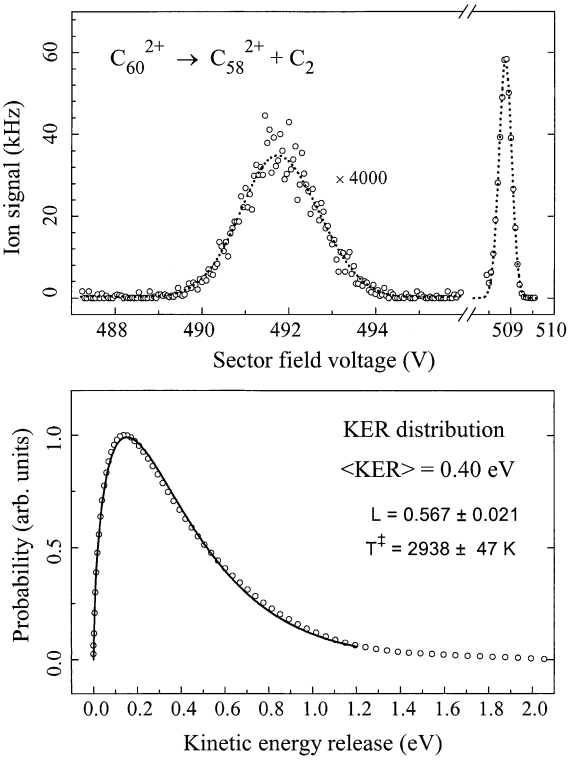

Fig. 6. Results pertaining to decay of C_{60}^{2+} into C_{58}^{2+}. Upper panel: parent ion peak at 509 V, and MIKE spectra showing raw data (open circles) and smoothed data (dotted line). Lower panel, open circles: KER distribution derived from the deconvoluted MIKE spectrum. Solid line: nonlinear least-squares fit of Eq. (4) to the experimental KER distribution.

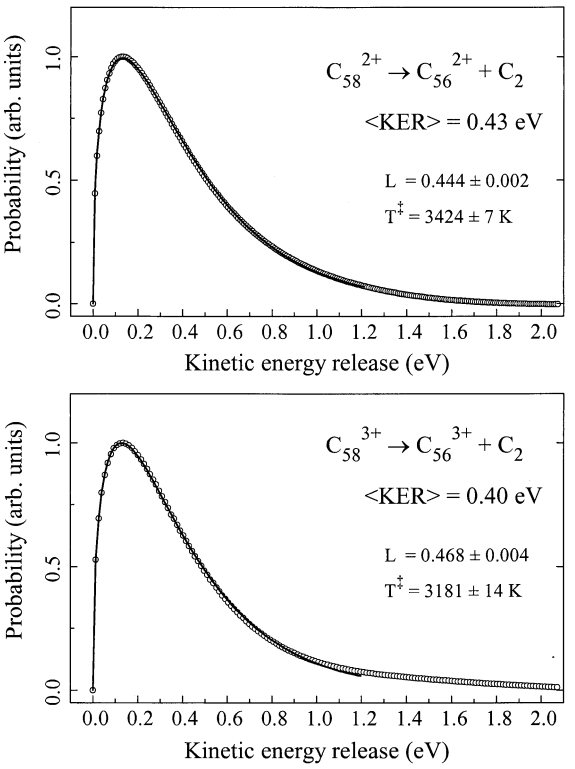

Fig. 7. Results pertaining to decay of C_{58}^{2+} and C_{58}^{3+}. Open circles: experimental KER distribution; solid line: nonlinear least-squares fit of Eq. (4) to the experimental KER distribution.

6. Kinetic energy release distributions of metastable fullerene ions

We have recorded MIKE spectra for metastable decay of singly and multiply charged C_{60} and C_{70} ions, and for metastable decay of C_{58} ions formed in the ion source from C_{60} parent ions. Singly, doubly, and triply charged C_{58} and C_{60} ions were recorded with the same high resolution as the C_3H_8 and C_3H_7 spectra (β slit width 0.2 mm); they were analyzed in the same way. Fig. 6 shows, as an example, the results for C_{60}^{2+}. The upper panel shows (open dots) that the parent ions peak at 509 V and that the MIKE spectrum is about six times broader than the former. The FFT-filtered MIKE spectrum is deconvoluted with a Gaussian fitted to the parent ion peak (dotted lines), and transformed into a KER distribution (lower panel, open circles). Only the left half of the MIKE peak is used in this procedure because the high-energy side may suffer from artifacts [26]. A generalized Maxwell–Boltzmann function [Eq. (4)] is then fitted to the distribution (solid line). It is straightforward to show that the average KER of the distribution is $\bar{\epsilon} = (1 + l)\ T^{\ddagger}$. For the spectrum shown in Fig. 6 we thus obtain a value of 0.40 eV.

Two more examples, the KER distributions of C_{58}^{2+} and C_{58}^{3+}, are shown in Fig. 7. In this case, Eq. (4) provides an almost perfect fit to the data. This attests to the absence of a reverse activation barrier for these species, in agreement with earlier studies pertaining to C_{60}^{+} [5,10]. For C_{58}^{z+} we have recorded and analyzed three or four spectra for each charge state ($z = 1$–3). The variations of the results are small for $z = 2$ and 3, but the reproducibility for the singly charged ions is

rather poor. Likewise, the quality of the C_{60}^{+} spectra is significantly poorer than that for C_{60}^{2+} and C_{60}^{3+}. This problem may be partly related to the fact that the singly charged fullerenes in general, and C_{60}^{+} in particular, have rather small metastable fractions [31], thus limiting the statistical accuracy of their MIKE spectra.

Deriving the average KER from the KER distribution lends the advantage that the MIKE peak does not have to be of Gaussian shape. Also, a separate determination of the parameters l and $T^{\ddagger}$ provides more information about the activation energy for dissociation than $\bar{\epsilon}$ would [16,17]; this will be discussed elsewhere [32]. On the other hand, This kind of data analysis is not a robust procedure; considerable errors may arise from the FFT filtering of random noise, the deconvolution procedure, an incorrect choice of the centroid of the MIKE peak, or a sloped background under the MIKE peak. In the following, we will attempt to quantify these errors.

Fortunately, reactions (1)–(3) are not affected by any significant background; the left, low-energy tails of the MIKE peaks properly converge to zero. Furthermore, the parent ion peaks are considerably narrower than the MIKE peaks, hence the deconvolution will not cause significant distortions. The effect of the other factors is explored in Fig. 8, based on the MIKE spectrum of C_{60}^{2+} shown before. In the top panel we plot the relative change of the parameters l, $T^{\ddagger}$, and $\bar{\epsilon} = (1 + l)T^{\ddagger}$ versus the number of points used in the FFT filtering routine. Strong smoothing (large number of points) results in broadening of the MIKE peak and a concomitant increase in $T^{\ddagger}$ and $\bar{\epsilon}$. The smooth curve displayed in Fig. 6 (top) is based on an FFT filter comprising 19 points; Fig. 8 suggests that this may lead to an overestimate of $\bar{\epsilon}$ by about 6%. The effect on $T^{\ddagger}$ would be 2%.

The uncertainty in determining the centroid of the MIKE peak is about 0.05 V, corresponding to the interval between adjacent data points in the MIKE spectrum. The middle panel in Fig. 8 suggests that this uncertainty translates to an uncertainty of 4% for $\bar{\epsilon}$, and 2% for $T^{\ddagger}$ (relative to the values obtained at a voltage of 491.80 V, upon which the KER distribution displayed in Fig. 6 is based).

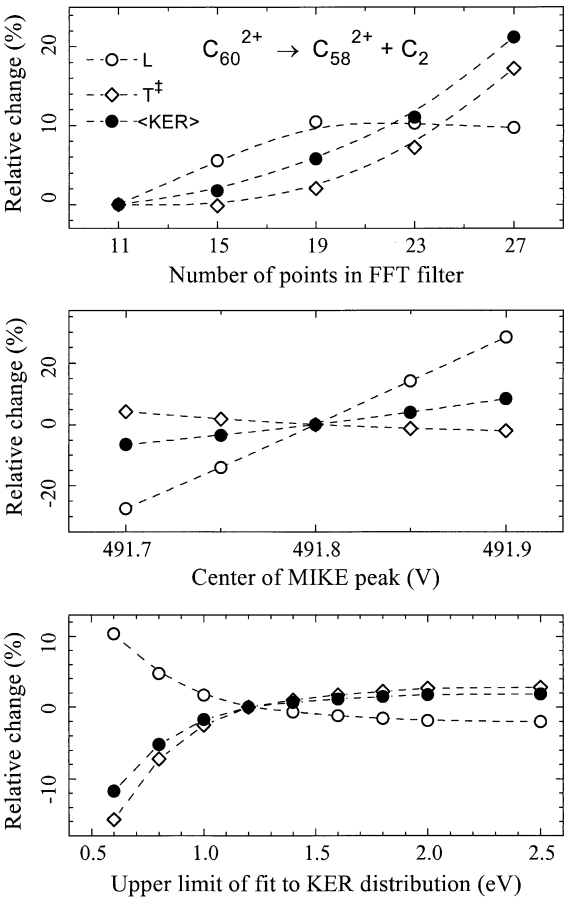

Fig. 8. Assessing the effects that the degree of smoothing, the choice of the centroid of the MIKE peak, and the upper limit in the fit to the KER distribution will have on the values of l (open circles), $T^{\ddagger}$ (open diamonds), and the average KER (solid circles). These data pertain to the decay of C_{60}^{2+} into C_{58}^{2+}.

Finally, the result of fitting a Maxwellian [Eq. (4)] to the experimental KER distribution will also depend on the range over which the fit is executed, as revealed in the bottom panel of Fig. 8. The data are referenced to values obtained with a KER limit of 1.2 eV, as used in Fig. 6. Extending the fit to larger KER values would not change $T^{\ddagger}$ and $\bar{\epsilon}$ by more than a few percent.

Summarizing, Fig. 8 suggests that the data analysis may possibly introduce systematic errors of about 10% in the values of $T^{\ddagger}$ and $\bar{\epsilon}$, whereas the parameter l may carry a much larger error. Although the values were obtained from a specific MIKE spectrum, further

Table 1
Experimental results. Column 2 summarizes the average kinetic energy release, $\bar{\epsilon}$, obtained through the model free approach [fit of Eq. (4) to the KER distribution]. Column 3 shows $\bar{\epsilon}$ obtained via a Gaussian fit to the MIKE peak. Previously published data are compiled in column 4

Parent	$\bar{\epsilon}$ (eV)	$\bar{\epsilon}$ (eV)	$\bar{\epsilon}$ (eV)
C_{58}^{+}	0.46 ± 0.12[a]	0.43	0.4 ± 0.1[c]
C_{58}^{2+}	0.44 ± 0.03[a]	0.42	
C_{58}^{3+}	0.40 ± 0.01[a]	0.42	
C_{60}^{+}	0.40	0.41	0.4 ± 0.1[c], 0.43 ± 0.05[d], 0.362[e], 0.45 ± 0.09[f]
C_{60}^{2+}	0.40	0.41	0.57 ± 0.20[f], 0.415 ± 0.05[d]
C_{60}^{3+}	0.44	0.41	0.43[g]
C_{60}^{4+}		0.41[b]	
C_{70}^{+}		0.49	0.370[e]
C_{70}^{2+}		0.45	
C_{70}^{3+}		0.49	
C_{70}^{4+}		0.47[b]	

[a] Average of three or four values, with standard deviation.
[b] Extrapolated, see text.
[c] [5].
[d] [6].
[e] [8].
[f] [11].
[g] [37].

analysis shows that they are also representative of our spectra for decay of C_{60}^{3+}, C_{58}^{2+}, and C_{58}^{3+}. However, the quality of our data for C_{60}^{+} and, in particular, C_{58}^{+}, is poorer, partly because their metastable fractions are lower [31].

The results discussed so far are compiled in the second column of Table 1. Experimental errors (standard deviations) are derived in those cases where several independent data sets were available. Given that the additional, systematic errors may possibly amount to 10%, we do not assign any significance to the differences found for fullerenes of different size or charge state. The third column lists the results obtained by a less elaborate but more robust procedure: Instead of FFT filtering the raw data, a Gaussian curve is fitted to the MIKE peak (under exclusion of the high-energy side of the peak). This function is then deconvoluted and transformed to a KER distribution from which the average KER is obtained. The agreement with the results obtained by the other method is within 0.03 eV.

The latter method was also applied to MIKE spectra of C_{70}^{z+}, $z = 1$–3; results are included in the third column of Table 1. Their average KER values tend to be larger than those of C_{58}^{z+} and C_{60}^{z+} ions by about 0.05 eV. This, if statistically significant, would indicate a slightly higher dissociation energy for C_{70}^{z+}, even if its larger number of degrees of freedom are taken into account [16]. An increase in the dissociation energy would be in agreement with recent experimental data by Matt et al. [33], but at variance with results of other workers [34, 35]. A detailed discussion of dissociation energies extracted from the present data will be published elsewhere [32].

Table 1 also lists the average KER for quadruply charged C_{60} and C_{70} ions. These values are derived indirectly from MIKE spectra recorded earlier with a wider β slit [36]. Under those conditions we consistently obtained values that appeared to increase linearly with the charge state. We have explored the effect of the slit width on the apparent average KER and corrected the values for C_{60}^{4+} and C_{70}^{4+} accordingly. In the limit of narrow slits, we find no systematic dependence of the average KER on the charge state of the fullerene ions.

Acknowledgements

This work was partially supported by the Österreichischer Fonds zur Förderung der Wissenschaftlichen Forschung, the Bundesministerium für Wissenschaft und Verkehr and the Jubiläumsfonds der Österreichischen Nationalbank, Wien, and the Fonds zur verstärkten Förderung von wissenschaftlichen Auslandsbeziehungen, Leopold Franzens Universität, Innsbruck. Work at the Hebrew University was supported by The Austrian Friends of The Hebrew University. The Farkas Research Center is supported by the Minerva Gesellschaft für die Forschung GmbH, München.

References

[1] T.D. Märk, O. Echt, in Clusters of Atoms and Molecules II, H. Haberland (Ed.), Springer-Verlag, Berlin, 1994, Vol. 56, p. 154.

[2] A.J. Stace, J. Chem. Phys. 85 (1986) 5774.
[3] C. Lifshitz, F. Louage, Int. J. Mass Spectrom. Ion Processes 101 (1990) 101.
[4] S. Wei, W.B. Tzeng, A.W. Castleman, J. Chem. Phys. 92 (1990) 332.
[5] R.P. Radi, H. Ming-Teh, M.E. Rincon, P.R. Kemper, M.T. Bowers, Chem. Phys. Lett. 174 (1990) 223.
[6] C. Lifshitz, M. Iraqi, T. Peres, J.E. Fischer, Int. J. Mass Spectrom. Ion Processes 107 (1991) 565.
[7] P. Sandler, T. Peres, G. Weissman, C. Lifshitz, Ber. Bunsenges. Phys. Chem. 96 (1992) 1995.
[8] P. Sandler, C. Lifshitz, C.E. Klots, Chem. Phys. Lett. 200 (1992) 445.
[9] C. Lifshitz, P. Sandler, H.F. Grützmacher, J. Sun, T. Weiske, H. Schwarz, J. Phys. Chem. 97 (1993) 6592.
[10] J. Laskin, C. Weickhardt, C. Lifshitz, Int. J. Mass Spectrom. Ion Processes 161 (1997) L7.
[11] T. Rauth, O. Echt, P. Scheier, T.D. Märk, Chem. Phys. Lett. 247 (1995) 515.
[12] A.J. Stone, D.J. Wales, Chem. Phys. Lett. 128 (1986) 501.
[13] C. Lifshitz, Mass Spectrom. Rev. 12 (1993) 261.
[14] G.E. Scuseria, Science, 271 (1996) 942.
[15] P.C. Engelking, J. Chem. Phys. 87 (1987) 936.
[16] C.E. Klots, Z. Phys. D 20 (1991) 105.
[17] C.E. Klots, J. Polach, J. Phys. Chem. 99 (1995) 15 396.
[18] R. Wörgötter, J. Kubista, J. Zabka, Z. Dolojsek, T.D. Märk, Z. Herman, Int. J. Mass Spectrom. Ion Processes 174 (1998) 53.
[19] M. Medved, R.G. Cooks, J.H. Beynon, Int. J. Mass Spectrom. Ion Processes 19 (1976) 179. The authors report three values recorded at different vapor temperatures, with an average of 2.16×4.47 meV, where the factor 2.16 is used to convert their FWHM values to the average KER.
[20] J.L. Holmes, A.D. Osborne, G.M. Weese, Int. J. Mass Spectrom. Ion Processes 19 (1976) 207.
[21] J.L. Holmes, A.D. Osborne, Int. J. Mass Spectrom. Ion Processes 23 (1977) 189.
[22] R.G. Cooks, J.H. Beynon, R.M. Caprioli, G.R. Lester, Metastable Ions, Elsevier, Amsterdam, 1973.
[23] J.E. Szulejko, A. Mendez Amaya, R.P. Morgan, A.G. Brenton, J.H. Beynon, Proc. R. Soc. London, Ser. A 373 (1980) 1.
[24] M.F. Jarrold, J. Illies, N.J. Kirchner, W. Wagner-Redeker, M.T. Bowers, M.L. Mandich, J.L. Beauchamp, J. Phys. Chem. 87 (1983) 2213.
[25] To be exact, the height of the rectangle will be modulated by a factor $1 \pm u_2/\nu_1$. We ignore this effect because under our conditions, for dissociation of fullerenes [reactions (1)–(3)] with a KER of about 0.4 eV, we have $\langle u_2 \rangle / \nu_1 \approx 0.002$.
[26] B.A. Rumpf, P.J. Derrick, Int. J. Mass Spectrom. Ion Processes 82 (1988) 239.
[27] D.A. Dahl, in Proceedings of the 43rd ASMS Conference on Mass Spectrometry and Allied Topics, Atlanta, GA, May 1995, p. 717.
[28] P. Scheier, G. Senn, S. Matt, T.D. Märk, Int. J. Mass Spectrom. Ion Processes 172 (1998) L1.
[29] W.H. Press, B.P. Flannery, S.A. Teukolsky, W.T. Vetterling, Numerical Recipes—The Art of Scientific Computing, Cambridge University Press, Cambridge, 1989.
[30] J.L. Holmes, A.D. Osborne, Org. Mass Spectrom. 13 (1978) 133.
[31] M. Foltin, O. Echt, P. Scheier, B. Dünser, R. Wörgötter, D. Muigg, S. Matt, T.D. Märk, J. Chem. Phys. 107 (1997) 6246.
[32] S. Matt, O. Echt, M. Sonderegger, R. David, P. Scheier, J. Laskin, C. Lifshitz, T.D. Märk, Chem. Phys. Lett., in press.
[33] S. Matt, O. Echt, R. Wörgötter, P. Scheier, C.E. Klots, T.D. Märk, Int. J. Mass Spectrom. Ion Processes 167/168 (1997) 753.
[34] C.E. Klots, Z. Phys. D 21 (1991) 335.
[35] P.E. Barran, S. Firth, A.J. Stace, H.W. Kroto, K. Hansen, E.E.B. Campbell, Int. J. Mass Spectrom. Ion Processes 167/168 (1997) 127.
[36] S. Matt, Ph.D. thesis, Leopold-Franzens Universität Innsbruck, 1998.
[37] C. Lifshitz, unpublished results.